

Robust stability of event-triggered nonlinear moving horizon estimation

Isabelle Krauss, Victor G. Lopez, *Member, IEEE*, and Matthias A. Müller, *Senior Member, IEEE*

Abstract—In this work, we propose an event-triggered moving horizon estimation (ET-MHE) scheme for the remote state estimation of general nonlinear systems. In the presented method, whenever an event is triggered, a single measurement is transmitted and the nonlinear MHE optimization problem is subsequently solved. If no event is triggered, the current state estimate is updated using an open-loop prediction based on the system dynamics. Moreover, we introduce a novel event-triggering rule under which we demonstrate robust global exponential stability of the ET-MHE scheme, assuming a suitable detectability condition is met. In addition, we show that with the adoption of a varying horizon length, a tighter bound on the estimation error can be achieved. Finally, we validate the effectiveness of the proposed method through two illustrative examples.

Index Terms—Moving horizon estimation, event-triggered state estimation, incremental system properties, nonlinear systems

I. INTRODUCTION

Moving horizon estimation (MHE) is a state estimation method that works by minimizing a cost function that considers past measurements. This method has proven to be a powerful solution to the state estimation problem due to its applicability to general nonlinear and potentially constrained systems subject to model inaccuracies and measurement noise. Furthermore, strong theoretical guarantees such as robust stability properties have been shown under a mild detectability condition (incremental input/output-to-state stability (i-IOSS)), cf. [4], [7], [10], [17], [20]. In certain applications, limited resources such as computation power, energy, and communication bandwidth present significant challenges. For example, networked control systems that are composed of numerous interconnected devices (e.g., sensors and actuators), often face bandwidth constraints that hinder simultaneous data transmission [26]. Moreover, in many applications it is desirable to conserve the energy of battery-operated devices [1]. Event-triggered methods can be employed to address these challenges by reducing the amount of unnecessary transmissions, see e.g. [6], [18].

For linear systems, significant progress has been made in event-triggered, optimization-based state estimation. An

This work received funding from the European Research Council (ERC) under the European Union's Horizon 2020 research and innovation programme (grant agreement No 948679).

I. Krauss, V. G. Lopez and M. A. Müller are with the Leibniz University Hannover, Institute of Automatic Control, 30167 Hannover, Germany {krauss, lopez, mueller}@irt.uni-hannover.de

event-triggered maximum likelihood estimation method for detectable systems under Gaussian noise was proposed in [21]. Furthermore, in works such as [24], [25] and [15] event-triggered moving horizon estimation (ET-MHE) schemes were developed that guarantee boundedness of the estimation error for observable systems subject to bounded disturbances.

In the context of nonlinear systems, adaptations of the Kalman filter form the basis for several event-triggered state estimation methods. For instance, a cubature Kalman filter with a deterministic event-triggering rule was presented in [13]. Additionally, stochastic event-triggering mechanisms in unscented and cubature Kalman filters are proposed in [16] and [14], where stochastic stability of the estimator is shown under certain observability assumptions. Other event-triggered state estimation methods for specific classes of nonlinear systems have also been proposed in the literature. For instance, state-affine systems are considered in [5], while an event-triggered impulse observer for nonlinear Lipschitz systems is presented in [22]. Moreover, a nonlinear MHE for networked systems featuring sector-bounded nonlinear dynamics and linear output functions, using a so-called random access protocol to schedule data transmission, has been described in [26].

In [11], we introduced a robustly stable event-triggered moving horizon estimation (ET-MHE) scheme for remote state estimation of general nonlinear detectable systems. In that work, the optimization problem is required to be explicitly solved only when an event occurs. This approach not only reduces the computational complexity of the method but also reduces the frequency with which the communication channel between the plant and a remote estimator is accessed. However, the method in [11] requires to transmit a (potentially long) sequence of measurements to the remote estimator when an event is triggered. This was required to show robust stability of the state estimation scheme.

In this paper, we now propose an ET-MHE scheme that only needs to send one measurement instead of a sequence of measurements to the remote side. Hence, it not only reduces how often the communication channel needs to be accessed, but also can potentially largely reduce the amount of data that needs to be sent in comparison with [11]. For the proposed method we establish robust global exponential stability (RGES) of the estimation error with respect to disturbances and noise. Furthermore, we show how to modify the proposed ET-MHE by considering a varying horizon length, such that our theoretical analysis leads to a tighter bound on the estimation error.

The rest of the paper is organized as follows. In Section II we explain the setting of this work and provide some technical definitions. In Section III the ET-MHE scheme is presented. We formulate the optimization problem and propose the event-triggering mechanism (ETM) used in the algorithm. This is followed by the stability analysis of the proposed scheme in Section IV. There, we show robust stability of the proposed ET-MHE scheme under a suitable detectability assumption. In Section V we extend the ET-MHE scheme proposed in Section III such that a varying horizon length is used, resulting in tighter error bounds. Here, we again establish RGES of the estimator. Finally, Section VI presents simulation examples to illustrate the effectiveness of the proposed method.

II. PRELIMINARIES AND PROBLEM SETUP

We denote the set of all nonnegative real numbers by $\mathbb{R}_{\geq 0}$. The set of integers within the interval $[a, b]$ for some $a, b \in \mathbb{R}$ is represented by $\mathbb{I}_{[a, b]}$, while $\mathbb{I}_{\geq a}$ denotes the set of integers greater than or equal to a for some $a \in \mathbb{R}$. The bold symbol \mathbf{u} refers to a sequence of the vector-valued variable $u \in \mathbb{R}^m$, $\mathbf{u} = \{u_0, u_1, \dots\}$ and the notation $(\mathbb{R}^m)^\infty$ denotes the set of all sequences \mathbf{u} with infinite length. The Euclidean norm of a vector $x \in \mathbb{R}^n$ is denoted by $\|x\|$. Additionally, we denote $\|x\|_P^2 = x^\top P x$ where P is a symmetric and positive definite matrix. The symbols $\lambda_{\min}(P)$ and $\lambda_{\max}(P)$ represent the minimum and maximum eigenvalues of the matrix P , respectively, while $\lambda_{\max}(P, Q)$ denotes the maximum generalized eigenvalue for the positive definite matrices P and Q . Lastly, $P \succ 0$ and $P \succeq 0$ indicate that a matrix P is positive definite and positive semi-definite, respectively.

We consider the discrete-time nonlinear system

$$\begin{aligned} x_{t+1} &= f(x_t, u_t, w_t) \\ y_t &= h(x_t, u_t, w_t) \end{aligned} \quad (1)$$

with state $x_t \in \mathbb{X} \subseteq \mathbb{R}^n$, control input $u_t \in \mathbb{U} \subseteq \mathbb{R}^m$, process disturbance and measurement noise¹ $w_t \in \mathbb{W} \subseteq \mathbb{R}^q$ with $0 \in \mathbb{W}$, noisy output measurement $y_t \in \mathbb{Y} \subseteq \mathbb{R}^p$, time $t \in \mathbb{I}_{\geq 0}$, and nonlinear continuous functions $f : \mathbb{X} \times \mathbb{U} \times \mathbb{W} \rightarrow \mathbb{X}$, $h : \mathbb{X} \times \mathbb{U} \times \mathbb{W} \rightarrow \mathbb{Y}$ representing the system dynamics and the output model, respectively².

To design a robustly stable MHE, it is necessary to make a suitable detectability assumption about the system. As we aim for robust global exponential stability, we use exponential i-IOSS as the detectability criterion.

Assumption 1 (Exponential i-IOSS): The system (1) is exponentially i-IOSS, i.e., there exist $P_1, P_2 \succ 0$, $Q, R \succeq 0$ and $\eta \in [0, 1)$ such that for any pair of initial conditions $x_0, \tilde{x}_0 \in \mathbb{X}$ and any input trajectories $\mathbf{w}, \tilde{\mathbf{w}} \in \mathbb{W}^\infty$ and $\mathbf{u} \in \mathbb{U}^\infty$

¹Here we use w to denote both process and measurement noise. This is a more general formulation of the problem that includes, e.g., having separate additive disturbances as a special case.

²The sets $\mathbb{X}, \mathbb{W}, \mathbb{U}, \mathbb{Y}$ are inherently satisfied due to the physical nature of the system such as non-negativity of the absolute temperature, partial pressures, or concentrations of species in a chemical reaction, compare e.g. the discussion in [4, Section 3].

it holds for all $t \geq 0$

$$\begin{aligned} \|x_t - \tilde{x}_t\|_{P_1}^2 &\leq \|x_0 - \tilde{x}_0\|_{P_2}^2 \eta^t \\ &+ \sum_{j=0}^{t-1} \eta^{t-j-1} \|w_j - \tilde{w}_j\|_Q^2 \\ &+ \sum_{j=0}^{t-1} \eta^{t-j-1} \|y_j - \tilde{y}_j\|_R^2, \end{aligned} \quad (2)$$

where $x_{t+1} = f(x_t, u_t, w_t)$, $\tilde{x}_{t+1} = f(\tilde{x}_t, u_t, \tilde{w}_t)$ and $y_t = h(x_t, u_t, w_t)$, $\tilde{y}_t = h(\tilde{x}_t, u_t, \tilde{w}_t)$.

Note that exponential i-IOSS is a necessary condition for the existence of robustly exponentially stable state estimators (cf. [9, Prop. 3], [3, Prop. 2.6]). Adapting the converse Lyapunov theorem from [3] shows that Assumption 1 implies that system (1) admits a quadratically-bounded i-IOSS Lyapunov function $W_\delta(x, \tilde{x})$ such that, for all $x, \tilde{x} \in \mathbb{X}$, all $u \in \mathbb{U}$, all $w, \tilde{w} \in \mathbb{W}$ and all $y, \tilde{y} \in \mathbb{Y}$

$$\begin{aligned} \|x - \tilde{x}\|_{P_1}^2 &\leq W_\delta(x, \tilde{x}) \leq \|x - \tilde{x}\|_{P_2}^2, \\ W_\delta(f(x, u, w), f(\tilde{x}, u, \tilde{w})) \\ &\leq \eta W_\delta(x, \tilde{x}) + \|w - \tilde{w}\|_Q^2 + \|y - \tilde{y}\|_R^2 \end{aligned} \quad (3)$$

with $\eta \in [0, 1)$, $P_1, P_2 \succ 0$ and $Q, R \succeq 0$. A systematic approach for calculating an i-IOSS Lyapunov function is presented in [20, Section IV], thereby allowing for the systematic verification of Assumption 1.

In Section IV, we show that the proposed ET-MHE is robustly globally exponentially stable according to the following definition.

Definition 1 (RGES [8, Def. 1]): A state estimator for system (1) is robustly globally exponentially stable (RGES) if there exist $C_x, C_w > 0$ and $\lambda_x, \lambda_w \in [0, 1)$ such that for any initial conditions $x_0, \hat{x}_0 \in \mathbb{X}$ and any disturbance sequence $\mathbf{w} \in \mathbb{W}^\infty$ the resulting state estimate \hat{x}_t satisfies the following for all $t \geq 0$

$$\|x_t - \hat{x}_t\| \leq C_x \|x_0 - \hat{x}_0\| \lambda_x^t + \sum_{j=0}^{t-1} C_w \|w_j\| \lambda_w^{t-j-1}. \quad (4)$$

In this definition of RGES the influence of past disturbances on the error bound is discounted. As a result, the estimation error converges to zero when disturbances fade.

III. ET-MHE SCHEME

MHE is an optimization-based state estimation method that, at each time t , computes the current state estimate by solving an optimization problem defined over a window of past inputs and outputs. In this section, we propose an ET-MHE scheme in which, when the optimization problem is solved, it uses a fixed window length. An extension of this scheme, where the horizon length is allowed to vary, is presented in a subsequent section.

The ET-MHE scheme presented in this section works as follows. When there is an event, a single measurement sample is transmitted from the plant side to the remote estimator. The estimator then – and only then – solves the nonlinear optimization problem that yields the optimal state estimate.

We show that, when the optimization problem is not solved, an open-loop prediction provides the optimal state estimate.

The ETM is responsible for determining if an event is scheduled by computing the value of the binary event-triggering variable γ_t . If $\gamma_t = 1$, an event occurs and the output measurement³ y_{t-1} is sent to the estimator; $\gamma_t = 0$ indicates that there is no event and thus no data transmission at time t . The most recent time an event was scheduled before the current time t is denoted by $\epsilon_t := \max\{0 \leq \tau < t | \gamma_\tau = 1\}$. For simplicity, we set $\epsilon_0 = 0$ and $\gamma_0 = 1$. Furthermore, δ_t refers to the number of time steps that have passed since the last event, i.e.,

$$\delta_t = \begin{cases} t - \epsilon_t, & \gamma_t = 0 \\ 0, & \gamma_t = 1. \end{cases}$$

How the ETM schedules an event will be discussed in more detail below.

As remote estimator we consider an MHE with a window length $M_t = \min\{t, M + \delta_t\}$ with $M \in \mathbb{I}_{\geq 0}$.

Remark 1: Note that within our scheme, the MHE optimization problem is required to be explicitly solved only when an event is triggered (see Proposition 1 below). At those time instances $\delta_t = 0$, which implies that the horizon length is equal to M for $t \geq M$. Therefore, whenever the optimization problem is explicitly solved, it is exclusively solved with a fixed horizon length of M for $t \geq M$.

Notice that we still define a variable horizon M_t for all t because it simplifies our analysis of the proposed ET-MHE. We first show that solving the optimization problem at every time instance with variable horizon length is *equivalent* to solving the optimization problem only when there is an event, and using an open-loop prediction when there is no event. Then, we simply show robust stability of the former case (see Theorem 1).

Since in this scheme we only send a single measurement in case of an event, the MHE cannot access all the measurements in the estimation horizon. Therefore, we define the set K_s that contains the time instances of the measurements that were sent to the remote estimator, i.e., $K_s := \{\tau | \gamma_{\tau+1} = 1\}$. The overall ET-MHE framework is depicted in Figure 1.

The MHE's nonlinear program (NLP) for $t < \tilde{\tau}$ with $\tilde{\tau} := \min\{\tau | \gamma_\tau = 0\}$ is given by

$$\min_{\hat{x}_{t-M_t|t}, \hat{w}_{\cdot|t}} J(\hat{x}_{t-M_t|t}, \hat{w}_{\cdot|t}, \hat{y}_{\cdot|t}, t) \quad (5a)$$

$$\text{s.t. } \hat{x}_{j+1|t} = f(\hat{x}_{j|t}, u_j, \hat{w}_{j|t}), \quad j \in \mathbb{I}_{[t-M_t, t-1]}, \quad (5b)$$

$$\hat{y}_{j|t} = h(\hat{x}_{j|t}, u_j, \hat{w}_{j|t}), \quad j \in \mathbb{I}_{[t-M_t, t-1]}, \quad (5c)$$

$$\hat{w}_{j|t} \in \mathbb{W}, \hat{y}_{j|t} \in \mathbb{Y}, \quad j \in \mathbb{I}_{[t-M_t, t-1]}, \quad (5d)$$

$$\hat{x}_{j|t} \in \mathbb{X}, \quad j \in \mathbb{I}_{[t-M_t, t]} \quad (5e)$$

The estimated state for time j computed at the current time t is indicated by the notation $\hat{x}_{j|t}$. Analogously, $\hat{w}_{j|t}$ and $\hat{y}_{j|t}$ denote the estimated disturbances and outputs. The notations $\hat{x}_{\cdot|t}^*$, $\hat{w}_{\cdot|t}^*$ and $\hat{y}_{\cdot|t}^*$ refer to the optimal state, disturbance, and output sequences, respectively, that minimize the cost function

³Note that we send y_{t-1} when $\gamma_t = 1$ since we use the prediction form of MHE and thus optimize over the window $[t - M_t, t - 1]$ to obtain the current state estimate at time t (see e.g. [2, Chapter 3]).

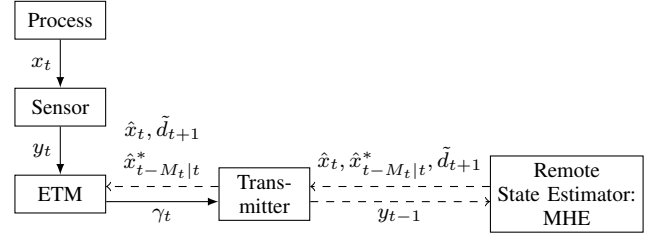


Fig. 1. Diagram of the overall ET-MHE framework. The dashed arrows represent the communication that is only required in case of an event.

J . The optimal estimate at the current time t is defined as $\hat{x}_t := \hat{x}_{t|t}^*$. Moreover, the notation $\hat{e}_t := x_t - \hat{x}_t$ is used to describe the estimation error at time t . For $t \geq \tilde{\tau}$, the MHE's NLP is given by (5) and the following additional constraint

$$\begin{aligned} & \sum_{j \in \mathbb{I}_{[t-M_t, \mu_t-1]} \setminus K_s} \eta^{\mu_t-j-1} \|\hat{y}_{j|t} - \tilde{y}_{j|\mu_t-1}\|_R^2 \\ & \leq \alpha \left(\sum_{j=\mu_t-M_{\mu_t}}^{\mu_t-1} \eta^{\mu_t-j-1} 2 \|\hat{w}_{j|\mu_t}^*\|_Q^2 \right. \\ & \quad \left. + \sum_{j \in \mathbb{I}_{[\mu_t-M_{\mu_t}, \mu_t-1]} \cap K_s} \eta^{\mu_t-j-1} \|\hat{y}_{j|\mu_t}^* - y_j\|_R^2 \right) \end{aligned} \quad (6)$$

with

$$\tilde{y}_{j|\mu_t-1} = \begin{cases} \hat{g}_{j|\mu_t-1}^*, & j < \mu_t - 1 \\ h(\hat{x}_{\mu_t-1}, u_{\mu_t-1}, 0), & j = \mu_t - 1. \end{cases}$$

The parameters α, η, Q, R correspond to the parameterization of the cost function (see below). The time instant μ_t , defined for $t \geq \tilde{\tau}$, refers to the last time when no event was triggered, i.e., $\mu_t := \max\{\tau | \tilde{\tau} \leq \tau \leq t, \gamma_\tau = 0\}$. Note also that $\mu_t - M_{\mu_t} = \epsilon_{\mu_t} - M_{\epsilon_{\mu_t}}$ since $\delta_{\epsilon_{\mu_t}} = 0$. The additional constraint is only required for $t \geq \tilde{\tau}$ since for $t < \tilde{\tau}$ the output y_t was transmitted at every time step. Consequently, the ET-MHE scheme corresponds to the non event-triggered MHE case for all $t < \tilde{\tau}$. As it will be shown in Section IV, the additional constraint (6) is a technical requirement that enables us to prove robust stability for the proposed scheme. We observed in numerical experiments (see Section VI) that this constraint did not affect the performance of the estimator in a significant way. This constraint can be interpreted as follows. The MHE optimization problem should drive the (complete) estimated output sequence towards meaningful values. At the times when there are measurements available, the estimated outputs should approach the measurements (this requirement is given by the cost function (7) below). At the times when there are no measurements available, the estimated outputs should be close to a previously obtained optimal output sequence. This is achieved by the constraint (6), which forces the left-hand side to be small depending on how accurate $\hat{y}_{j|\mu_t}^*$ was.

We consider the following cost function

$$\begin{aligned} J(\hat{x}_{t-M_t|t}, \hat{w}_{\cdot|t}, \hat{y}_{\cdot|t}, t) &= 2\eta^{M_t} \|\hat{x}_{t-M_t|t} - \hat{x}_{t-M_t}\|_{P_2}^2 \\ &+ \max\{1, \alpha\} \left(\sum_{j=t-M_t}^{t-1} \eta^{t-j-1} 2\|\hat{w}_{j|t}\|_Q^2 \right. \\ &\left. + \sum_{j \in \mathbb{I}_{[t-M_t, t-1]} \cap K_s} \eta^{t-j-1} \|\hat{y}_{j|t} - y_j\|_R^2 \right). \end{aligned} \quad (7)$$

The parameter $\alpha \geq 0$ is a design variable and corresponds to the sensitivity of the event-triggering condition, see Remark 3 below. The cost function consists of two parts, namely the prior weighting and the stage cost. The prior weighting penalizes the difference between the first element of the estimated state sequence $\hat{x}_{t-M_t|t}$ and the prior estimate \hat{x}_{t-M_t} that was obtained at time $t-M_t$. The estimated noise and the difference between the measured and the estimated output are penalized in the stage cost. The parameters P_2, Q, R and η correspond to the ones in Assumption 1. If the system is exponentially i-IOSS, then the cost function can be parameterized using any positive definite matrices P_2, Q and R (since (3) can be rescaled accordingly, cf. [20, Remark 1]). The discount factor η reduces the influence of disturbances and output measurements further in the past. A discounting MHE cost function was introduced in [8], and has proven particularly useful in the robust stability analysis of MHE.

Remark 2: In contrast to the cost function used in [11], this cost function (7) only considers measurements of time instances that are in K_s , rather than M consecutive measurements. Thus the output-dependent sum on the right-hand side of (7) consists of less elements. Another slight difference compared to the cost function in [11] is that we use the factor $\max\{1, \alpha\}$ instead of $(\alpha + 1)$ in the formulation of the stage costs. We want to remark here that both are possible formulations, however using $(\alpha + 1)$ would yield a larger error bound in the stability analysis in Section IV.

The following proposition from [11] is also applicable to the ET-MHE scheme proposed here and shows why it is sufficient to only solve the optimization problem at the time instances when an event occurs. When there is no event, the current estimate can be obtained using open-loop predictions. The proof requires only minor modifications to account for the fact that only measurements at time instances $t \in K_s$ are transmitted to the remote side. Nevertheless, we include it here for the sake of completeness.

Proposition 1 ([11, Proposition 1]): The solution of the NLP (5)-(6) at time $t \geq 0$ is given by

$$\hat{x}_{t-M_t|t}^* = \hat{x}_{t-\delta_t-M_{\delta_t}|t-\delta_t}^*, \quad (8a)$$

$$\hat{w}_{j|t}^* = \hat{w}_{j|t-\delta_t}^*, \quad j \in \mathbb{I}_{[t-M_t, t-\delta_t-1]}, \quad (8b)$$

$$\hat{w}_{j|t}^* = 0, \quad j \in \mathbb{I}_{[t-\delta_t, t-1]}. \quad (8c)$$

Proof: First, note that the last term of the cost function (7) only considers the time instances when the corresponding measurements were transmitted to the remote estimator, i.e., the measurements in $[t-M_t, t-\delta_t-1] \cap K_s$. Thus, $\hat{w}_{j|t} = 0$ for all $j \in [t-\delta_t, t-1]$ minimizes $J(\hat{x}_{t-M_t|t}, \hat{w}_{\cdot|t}, \hat{y}_{\cdot|t}, t)$.

Hence, the following holds for the optimal value of the cost function at time t

$$\begin{aligned} &J(\hat{x}_{t-M_t|t}^*, \hat{w}_{\cdot|t}^*, \hat{y}_{\cdot|t}^*, t) \\ &= \eta^{\delta_t} J(\hat{x}_{t-\delta_t-M_{\delta_t}|t-\delta_t}^*, \hat{w}_{\cdot|t-\delta_t}^*, \hat{y}_{\cdot|t-\delta_t}^*, t-\delta_t) \end{aligned}$$

where $t - \delta_t - M_{\delta_t} = t - M_t$ since $\delta_{t-\delta_t} = 0$. Thus, the solution obtained by minimizing $J(\hat{x}_{t-M_t|t}, \hat{w}_{\cdot|t}, \hat{y}_{\cdot|t}, t)$ is given by (8). \blacksquare

According to Proposition 1, if $\gamma_t = 0$, i.e., no event occurs, the estimates \hat{x}_j for all $j \in [t - \delta_t + 1, t]$ are given by an open-loop prediction

$$\hat{x}_j = f(\hat{x}_{j-1}, u_{j-1}, 0). \quad (9)$$

Consequently, the NLP (5) only needs to be explicitly solved when an event is triggered. Since $\gamma_t = 1$ implies $\delta_t = 0$, the NLP that must be solved explicitly has a fixed horizon length M for $t \geq M$, as discussed in Remark 1.

As we show later in the proof of Theorem 1, RGES can be established using the following ETM, that determines the value of the scheduling variable γ_t at each time

$$\gamma_t = \begin{cases} 0, & \text{if } \begin{aligned} &\sum_{j \in \mathbb{I}_{[\epsilon_t - M_{\epsilon_t}, \epsilon_t - 1]} \setminus K_s} \eta^{t-j-1} \|y_j - \hat{y}_{j|\epsilon_t}^*\|_R^2 \\ &+ \sum_{j=\epsilon_t}^{t-1} \eta^{t-j-1} \|y_j - h(\hat{x}_j, u_j, 0)\|_R^2 \\ &< \alpha \eta^{t-\epsilon_t} d_t \end{aligned} \\ 1, & \text{otherwise} \end{cases} \quad (10)$$

with $\alpha \in \mathbb{R}_{\geq 0}$ and

$$\begin{aligned} d_t &= 2 \sum_{j=\epsilon_t - M_{\epsilon_t}}^{\epsilon_t - 1} \eta^{\epsilon_t - 1 - j} \|\hat{w}_{j|\epsilon_t}^*\|_Q^2 \\ &+ \sum_{j \in \mathbb{I}_{[\epsilon_t - M_{\epsilon_t}, \epsilon_t - 1]} \setminus K_s} \eta^{\epsilon_t - 1 - j} \|y_j - \hat{y}_{j|\epsilon_t}^*\|_R^2. \end{aligned} \quad (11)$$

However, directly evaluating the condition above would require sending several estimated outputs back to the plant side. Hence, to reduce the amount of data transmitted, we modify the ETM (10) by exploiting the following bound

$$\begin{aligned} &\sum_{j \in \mathbb{I}_{[\epsilon_t - M_{\epsilon_t}, \epsilon_t - 1]} \setminus K_s} \eta^{t-j-1} \|y_j - \hat{y}_{j|\epsilon_t}^*\|_R^2 \\ &\leq 2 \sum_{j \in \mathbb{I}_{[\epsilon_t - M_{\epsilon_t}, \epsilon_t - 1]} \setminus K_s} \eta^{t-j-1} \|\bar{y}_j^{\epsilon_t} - \hat{y}_{j|\epsilon_t}^*\|_R^2 \\ &\quad + 2 \sum_{j \in \mathbb{I}_{[\epsilon_t - M_{\epsilon_t}, \epsilon_t - 1]} \setminus K_s} \eta^{t-j-1} \|y_j - \bar{y}_j^{\epsilon_t}\|_R^2 \end{aligned} \quad (12)$$

with $\bar{x}_{\epsilon_t - M_{\epsilon_t}}^{\epsilon_t} = \hat{x}_{\epsilon_t - M_{\epsilon_t}|\epsilon_t}$ and

$$\begin{aligned} \bar{x}_{j+1}^{\epsilon_t} &= f(\bar{x}_j^{\epsilon_t}, u_j, 0), \\ \bar{y}_j^{\epsilon_t} &= h(\bar{x}_j^{\epsilon_t}, u_j, 0), \quad j \in [\epsilon_t - M_{\epsilon_t}, \epsilon_t - 1]. \end{aligned}$$

We define

$$p_t = \sum_{j \in \mathbb{I}_{[\epsilon_t - M_{\epsilon_t}, \epsilon_t - 1]} \setminus K_s} \eta^{\epsilon_t - j - 1} \|\bar{y}_j^{\epsilon_t} - \hat{y}_{j|\epsilon_t}^*\|_R^2. \quad (13)$$

Algorithm 1 Event-triggered MHE

- 1: Set $\gamma_0 = 1$ and $\tilde{d}_1 = 0$.
- 2: Set $t = 1$.
- 3: ETM computes γ_t .
- 4: **if** $\gamma_t = 1$ **then**
- 5: y_{t-1} is sent to remote estimator.
- 6: NLP (5)-(7) of MHE is solved.
- 7: \tilde{d}_{t+1} is calculated
- 8: \tilde{d}_{t+1} , $\hat{x}_{t-M_t|t}^*$ and \hat{x}_t are sent back to the ETM.
- 9: **else**
- 10: \hat{x}_t is calculated according to (9).
- 11: $\hat{y}_t = h(\hat{x}_t, u_t, 0)$ is calculated.
- 12: Set $t = t + 1$ and go back to step 3.

Note that both d_t and p_t as defined in (11) and (13), respectively, can be calculated at the remote side since all required quantities to this end have been sent to the remote side. By sending additionally the first element of the estimated state sequence back to the plant side, $\bar{y}_j^{\epsilon_t}$ can be calculated at the plant side. Using (12) we can now formulate our event-triggering condition as follows

$$\gamma_t = \begin{cases} 2 \sum_{j \in \mathbb{I}_{[\epsilon_t - M_{\epsilon_t}, \epsilon_t - 1]} \setminus K_s} \eta^{t-j-1} \|y_j - \bar{y}_j^{\epsilon_t}\|_R^2 \\ 0, \text{ if } + \sum_{j=\epsilon_t}^{t-1} \eta^{t-j-1} \|y_j - h(\hat{x}_j, u_j, 0)\|_R^2 \\ \quad < \eta^{t-\epsilon_t} \tilde{d}_t \\ 1, \text{ otherwise} \end{cases} \quad (14)$$

where $\tilde{d}_t = (\alpha d_t - 2p_t)$. As previously stated, if $\gamma_t = 1$, the measurement y_{t-1} is transmitted to the remote state estimator and the optimization problem is solved at time t . Then, both d_{t+1} and p_{t+1} can be computed using the estimated disturbance and output sequences $\hat{w}_{\cdot|t}^*, \hat{y}_{\cdot|t}^*$ since $\epsilon_{t+1} = t$. Thereafter, \tilde{d}_{t+1} together with the first and the last element of the estimated state sequence, i.e., $\hat{x}_{t-M_t|t}^*$ and \hat{x}_t is sent back to the ETM to evaluate the triggering condition for the next time step (cf. Figure 1). Note that d_t and p_t , and thus \tilde{d}_t , are constant between events, i.e., $d_{t+1} = d_t$ and $p_{t+1} = p_t$ if $\gamma_t = 0$. This follows from (8) and the fact that $\epsilon_{t+1} = \epsilon_t$ if $\gamma_t = 0$. The steps of the ET-MHE scheme are outlined in Algorithm 1. Notice that in the algorithm we set $\tilde{d}_1 = 0$ and hence there is always an event triggered at time $t = 1$, i.e., the first measurement y_0 is sent to the remote side.

Remark 3: In the proposed method, α is a design parameter that affects the frequency of an event being triggered. When α is increased, the occurrence of events decreases, which consequently enlarges the disturbance gain in the error bound derived in Theorem 1 below.

Before we show robust stability of the proposed ET-MHE scheme in the following section, we want to conclude this section by making some remarks regarding the relations between the here proposed ET-MHE scheme and the method in [11].

Remark 4: Notice that, analogously to the method in [11], some scalar value (\tilde{d}_{t+1}) and the current state estimate (\hat{x}_t) are transmitted back to the plant side. Additionally, the first element of the estimated state sequence ($\hat{x}_{t-M_t|t}^*$) is now sent back. Hence, depending on the dimensions of the state and output and on the frequency of triggering, the total amount of data transmitted through the communication channel is not necessarily reduced compared to [11]. However, the proposed ET-MHE is generally expected to result in less data transmitted compared to the scheme in [11], since only a *single* measurement is sent to the remote estimator in case of an event. Notice, though, that due to the difference in the number of measurements transmitted and due to the bound (12), the inequality in the event-triggering condition (14) is in general more easily violated than its counterpart in [11] given the same value of α . Thus, α must be tuned accordingly to achieve a desired rate of triggering. Finally, notice that sending a single measurement per event is also advantageous compared to [11] in case of a large horizon length, since [11] could require transmitting many measurements in a single event.

IV. STABILITY ANALYSIS

Having introduced the ET-MHE scheme, this section now focuses on showing robust stability of the proposed method. The shift from transmitting a sequence of measurements, as in [11], to just a single measurement impacts the formulation of the stage cost. This change is the main reason why we had to fundamentally change the proof strategy compared to the robust stability proof in [11].

Theorem 1 (RGES of ET-MHE): Let Assumption 1 hold and the horizon $M \in \mathbb{I}_{\geq 0}$ be chosen such that $24\lambda_{\max}(P_2, P_1)\eta^M < 1$. Then there exists $\rho \in [0, 1)$ such that the state estimation error of the ET-MHE scheme (5)-(7) with $M_t = \min\{t, M + \delta_t\}$ and with the event scheduling condition (14) satisfies for all $t \geq 0$

$$\begin{aligned} \|\hat{e}_t\| &\leq \sqrt{\frac{24\lambda_{\max}(P_2)}{\lambda_{\min}(P_1)}} \sqrt{\rho^t} \|\hat{e}_0\| \\ &\quad + \sqrt{\frac{3 \max\{10\alpha + 2, 12\} \lambda_{\max}(Q)}{\lambda_{\min}(P_1)}} \sum_{j=0}^{t-1} \sqrt{\rho^{t-j-1}} \|w_j\|, \end{aligned}$$

i.e., the ET-MHE is an RGES estimator according to Definition 1.

Proof: Due to the constraints (5b)-(5e) in the NLP, at each time step t , the estimated trajectories satisfy (1), $\hat{x}_{j|t} \in \mathbb{X}$ for all $j \in \mathbb{I}_{[t-M_t, t]}$ and $\hat{w}_{j|t} \in \mathbb{W}$, $\hat{y}_{j|t} \in \mathbb{Y}$ for all $j \in \mathbb{I}_{[t-M_t, t-1]}$. Thus, we can apply (2) to obtain

$$\begin{aligned} \|\hat{x}_t - x_t\|_{P_1}^2 &\leq \eta^{M_t} \|\hat{x}_{t-M_t|t}^* - x_{t-M_t}\|_{P_2}^2 \\ &\quad + \sum_{j=t-M_t}^{t-1} \eta^{t-j-1} \|\hat{w}_{j|t}^* - w_j\|_Q^2 \\ &\quad + \sum_{j=t-M_t}^{t-1} \eta^{t-j-1} \|\hat{y}_{j|t}^* - y_j\|_R^2. \end{aligned}$$

Applying the Cauchy-Schwarz inequality, and Young's inequality, it holds that

$$\|\hat{w}_{j|t}^* - w_j\|_Q^2 \leq 2\|\hat{w}_{j|t}^*\|_Q^2 + 2\|w_j\|_Q^2$$

and therefore,

$$\begin{aligned} \|\hat{x}_t - x_t\|_{P_1}^2 &\leq \eta^{M_t} \|\hat{x}_{t-M_t|t}^* - x_{t-M_t}\|_{P_2}^2 \\ &\quad + \sum_{j=t-M_t}^{t-1} \eta^{t-j-1} 2\|w_j\|_Q^2 \\ &\quad + \sum_{j=t-M_t}^{t-1} \eta^{t-j-1} 2\|\hat{w}_{j|t}^*\|_Q^2 \\ &\quad + \sum_{j=t-M_t}^{t-1} \eta^{t-j-1} \|\hat{y}_{j|t}^* - y_j\|_R^2. \end{aligned}$$

Due to

$$\begin{aligned} &\|\hat{x}_{t-M_t|t}^* - x_{t-M_t}\|_{P_2}^2 \\ &= \|\hat{x}_{t-M_t} - x_{t-M_t} + \hat{x}_{t-M_t|t}^* - \hat{x}_{t-M_t}\|_{P_2}^2 \\ &\leq 2\|\hat{x}_{t-M_t} - x_{t-M_t}\|_{P_2}^2 + 2\|\hat{x}_{t-M_t|t}^* - \hat{x}_{t-M_t}\|_{P_2}^2 \end{aligned}$$

we can write

$$\begin{aligned} \|\hat{x}_t - x_t\|_{P_1}^2 &\leq 2\eta^{M_t} \|\hat{x}_{t-M_t} - x_{t-M_t}\|_{P_2}^2 \\ &\quad + 2\eta^{M_t} \|\hat{x}_{t-M_t|t}^* - \hat{x}_{t-M_t}\|_{P_2}^2 \\ &\quad + \sum_{j=t-M_t}^{t-1} \eta^{t-j-1} 2\|w_j\|_Q^2 \\ &\quad + \sum_{j=t-M_t}^{t-1} \eta^{t-j-1} 2\|\hat{w}_{j|t}^*\|_Q^2 \\ &\quad + \sum_{j \in \mathbb{I}_{[t-M_t, t-1]} \cap K_s} \eta^{t-j-1} \|\hat{y}_{j|t}^* - y_j\|_R^2 \\ &\quad + \sum_{j \in \mathbb{I}_{[t-M_t, t-1]} \setminus K_s} \eta^{t-j-1} \|\hat{y}_{j|t}^* - y_j\|_R^2. \end{aligned} \quad (15)$$

In the following, we aim to establish an upper bound for the last term in (15). If $t < \tilde{\tau}$, then the last term in (15) is an empty sum and thus zero. Therefore, it is sufficient to focus only on the case $t \geq \tilde{\tau}$. If $t \geq \tilde{\tau}$, then since μ_t refers to the last time no event was scheduled, it follows that the set $\mathbb{I}_{[t-M_t, t-1]} \setminus K_s$ is equal to the set $\mathbb{I}_{[t-M_t, \mu_t-1]} \setminus K_s$. Now, we can bound the last term of (15) as follows

$$\begin{aligned} &\sum_{j \in \mathbb{I}_{[t-M_t, \mu_t-1]} \setminus K_s} \eta^{t-j-1} \|\hat{y}_{j|t}^* - y_j\|_R^2 \\ &= \sum_{j \in \mathbb{I}_{[t-M_t, \mu_t-1]} \setminus K_s} \eta^{t-j-1} \|\hat{y}_{j|\mu_t}^* + \hat{y}_{j|\mu_t}^* - \hat{y}_{j|t}^*\|_R^2 \\ &\leq 2 \sum_{j \in \mathbb{I}_{[t-M_t, \mu_t-1]} \setminus K_s} \eta^{t-j-1} \|\hat{y}_{j|\mu_t}^*\|_R^2 \\ &\quad + 2 \sum_{j \in \mathbb{I}_{[t-M_t, \mu_t-1]} \setminus K_s} \eta^{t-j-1} \|\hat{y}_{j|\mu_t}^* - \hat{y}_{j|t}^*\|_R^2 \end{aligned} \quad (16)$$

From Proposition 1 and the facts that $\mu_t - \delta_{\mu_t} = \epsilon_{\mu_t}$ and $\epsilon_{\mu_t} - M_{\epsilon_{\mu_t}} \leq t - M_t$, we get

$$\begin{aligned} &2\eta^{t-\mu_t} \sum_{j \in \mathbb{I}_{[t-M_t, \mu_t-1]} \setminus K_s} \eta^{\mu_t-j-1} \|\hat{y}_{j|\mu_t}^* - y_j\|_R^2 \\ &= 2\eta^{t-\mu_t} \left(\sum_{j \in \mathbb{I}_{[t-M_t, \epsilon_{\mu_t}-1]} \setminus K_s} \eta^{\mu_t-j-1} \|\hat{y}_{j|\mu_t}^* - \hat{y}_{j|\epsilon_{\mu_t}}^*\|_R^2 \right. \\ &\quad \left. + \sum_{j=\epsilon_{\mu_t}}^{\mu_t-1} \eta^{\mu_t-j-1} \|\hat{y}_{j|\mu_t}^* - h(\hat{x}_j, u_j, 0)\|_R^2 \right) \\ &\leq 2\eta^{t-\mu_t} \left(\sum_{j \in \mathbb{I}_{[\epsilon_{\mu_t}-M_{\epsilon_{\mu_t}}, \epsilon_{\mu_t}-1]} \setminus K_s} \eta^{\mu_t-j-1} \|\hat{y}_{j|\mu_t}^* - \hat{y}_{j|\epsilon_{\mu_t}}^*\|_R^2 \right. \\ &\quad \left. + \sum_{j=\epsilon_{\mu_t}}^{\mu_t-1} \eta^{\mu_t-j-1} \|\hat{y}_{j|\mu_t}^* - h(\hat{x}_j, u_j, 0)\|_R^2 \right). \end{aligned}$$

If no event is triggered and thus the bound in (14) holds, then, by (12), the bound in (10) holds as well. Therefore, since no event is triggered at time μ_t , we obtain

$$\begin{aligned} &2\eta^{t-\mu_t} \sum_{j \in \mathbb{I}_{[t-M_t, \mu_t-1]} \setminus K_s} \eta^{\mu_t-j-1} \|\hat{y}_{j|\mu_t}^* - y_j\|_R^2 \\ &\leq 2\eta^{t-\mu_t} \left(\alpha \sum_{j=\mu_t-M_{\mu_t}}^{\epsilon_{\mu_t}-1} \eta^{\mu_t-j-1} 2\|\hat{w}_{j|\epsilon_{\mu_t}}^*\|_Q^2 \right. \\ &\quad \left. + \alpha \sum_{j \in \mathbb{I}_{[\mu_t-M_{\mu_t}, \epsilon_{\mu_t}-1]} \cap K_s} \eta^{\mu_t-j-1} \|\hat{y}_{j|\epsilon_{\mu_t}}^* - y_j\|_R^2 \right) \end{aligned} \quad (17)$$

where we used the fact that $\mu_t - M_{\mu_t} = \epsilon_{\mu_t} - M_{\epsilon_{\mu_t}}$.

Now we want to upper bound $2 \sum_{j \in \mathbb{I}_{[t-M_t, \mu_t-1]} \setminus K_s} \eta^{t-j-1} \|\hat{y}_{j|\mu_t}^* - \hat{y}_{j|t}^*\|_R^2$, i.e., the second term on the right-hand side of (16). For $\mu_t \leq t - M_t$ the sum is empty and thus $2 \sum_{j \in \mathbb{I}_{[t-M_t, \mu_t-1]} \setminus K_s} \eta^{t-j-1} \|\hat{y}_{j|\mu_t}^* - \hat{y}_{j|t}^*\|_R^2 = 0$. For $\mu_t > t - M_t$ notice that due to $\gamma_{\mu_t} = 0$, $\mu_{t-1} \notin K_s$ and hence we can apply the same argument as in the proof of Proposition 1 to conclude that $\hat{y}_{j|\mu_t}^* = \hat{y}_{j|\mu_t-1}^*$ for $j \in \mathbb{I}_{[t-M_t, \mu_t-2]}$ and $\hat{w}_{\mu_t-1|\mu_t}^* = 0$. Thus, we obtain

$$\begin{aligned} &2 \sum_{j \in \mathbb{I}_{[t-M_t, \mu_t-1]} \setminus K_s} \eta^{t-j-1} \|\hat{y}_{j|\mu_t}^* - \hat{y}_{j|t}^*\|_R^2 \\ &= 2\eta^{t-\mu_t} \sum_{j \in \mathbb{I}_{[t-M_t, \mu_t-2]} \setminus K_s} \eta^{\mu_t-j-1} \|\hat{y}_{j|\mu_t-1}^* - \hat{y}_{j|t}^*\|_R^2 \\ &\quad + 2\eta^{t-\mu_t} \|\hat{y}_{\mu_t-1|t}^* - h(\hat{x}_{\mu_t-1}, u_{\mu_t-1}, 0)\|_R^2. \end{aligned}$$

Hence, by constraint (6) we can write

$$\begin{aligned} &2 \sum_{j \in \mathbb{I}_{[t-M_t, \mu_t-1]} \setminus K_s} \eta^{t-j-1} \|\hat{y}_{j|\mu_t}^* - \hat{y}_{j|t}^*\|_R^2 \\ &\leq 2\eta^{t-\mu_t} \left(\alpha \sum_{j=\mu_t-M_{\mu_t}}^{\epsilon_{\mu_t}-1} \eta^{\mu_t-j-1} 2\|\hat{w}_{j|\epsilon_{\mu_t}}^*\|_Q^2 \right. \\ &\quad \left. + \alpha \sum_{j \in \mathbb{I}_{[\mu_t-M_{\mu_t}, \epsilon_{\mu_t}-1]} \cap K_s} \eta^{\mu_t-j-1} \|\hat{y}_{j|\epsilon_{\mu_t}}^* - y_j\|_R^2 \right). \end{aligned} \quad (18)$$

Substituting (17) and (18) in (16) and exploiting Proposition 1,

we obtain

$$\begin{aligned}
& \sum_{j \in \mathbb{I}_{[t-M_t, \mu_t-1]} \setminus K_s} \eta^{t-j-1} \|y_j - \hat{y}_{j|t}^*\|_R^2 \\
& \leq 4\eta^{t-\mu_t} \alpha \left(\sum_{j=\mu_t-M_{\mu_t}}^{\mu_t-1} \eta^{\mu_t-j-1} 2\|\hat{w}_{j|\mu_t}^*\|_Q^2 \right. \\
& + \left. \sum_{j \in \mathbb{I}_{[\mu_t-M_{\mu_t}, \mu_t-1]} \cap K_s} \eta^{\mu_t-j-1} \|\hat{y}_{j|\mu_t}^* - y_j\|_R^2 \right) \\
& \leq 4\eta^{t-\mu_t} J(\hat{x}_{\mu_t-M_{\mu_t}|\mu_t}^*, \hat{w}_{\cdot|\mu_t}^*, \hat{y}_{\cdot|\mu_t}, \mu_t) \\
& \leq 4\eta^{t-\mu_t} J(x_{\mu_t-M_{\mu_t}}, w_{\cdot|\mu_t}, y_{\cdot|\mu_t}, \mu_t)
\end{aligned} \tag{19}$$

where $w_{\cdot|\tau}$ and $y_{\cdot|\tau}$ refer to the true disturbance and output trajectories on the interval $[\tau - M_\tau, \tau - 1]$. Moreover, we can upper bound the following terms of (15) as follows

$$\begin{aligned}
& 2\eta^{M_t} \|\hat{x}_{t-M_t|t}^* - \hat{x}_{t-M_t}\|_{P_2}^2 + \sum_{j=t-M_t}^{t-1} \eta^{t-j-1} 2\|\hat{w}_{j|t}^*\|_Q^2 \\
& + \sum_{j \in \mathbb{I}_{[t-M_t, t-1]} \cap K_s} \eta^{t-j-1} \|\hat{y}_{j|t}^* - y_j\|_R^2 \\
& \leq J(\hat{x}_{t-M_t|t}^*, \hat{w}_{\cdot|t}^*, \hat{y}_{\cdot|t}, t) \leq J(x_{t-M_t}, w_{\cdot|t}, y_{\cdot|t}, t).
\end{aligned} \tag{20}$$

Substituting (19) and (20) in (15) results in

$$\begin{aligned}
\|\hat{e}_t\|_{P_1}^2 &= \|\hat{x}_t - x_t\|_{P_1}^2 \\
&\leq 4\eta^{M_t} \|\hat{x}_{t-M_t} - x_{t-M_t}\|_{P_2}^2 \\
&+ 8\eta^{t-\mu_t+M_{\mu_t}} \|\hat{x}_{\mu_t-M_{\mu_t}} - x_{\mu_t-M_{\mu_t}}\|_{P_2}^2 \\
&+ \max\{2\alpha + 2, 4\} \sum_{j=t-M_t}^{t-1} \eta^{t-j-1} \|w_j\|_Q^2 \\
&+ \max\{8\alpha, 8\} \sum_{j=\mu_t-M_{\mu_t}}^{\mu_t-1} \eta^{t-j-1} \|w_j\|_Q^2 \\
&\leq 4\eta^{M_t} \|\hat{x}_{t-M_t} - x_{t-M_t}\|_{P_2}^2 \\
&+ 8\eta^{t-\mu_t+M_{\mu_t}} \|\hat{x}_{\mu_t-M_{\mu_t}} - x_{\mu_t-M_{\mu_t}}\|_{P_2}^2 \\
&+ \max\{10\alpha + 2, 12\} \sum_{j=\mu_t-M_{\mu_t}}^{t-1} \eta^{t-j-1} \|w_j\|_Q^2 \\
&\leq \max\{12\eta^{M_t} \|\hat{x}_{t-M_t} - x_{t-M_t}\|_{P_2}^2, \\
&24\eta^{t-\mu_t+M_{\mu_t}} \|\hat{x}_{\mu_t-M_{\mu_t}} - x_{\mu_t-M_{\mu_t}}\|_{P_2}^2, \\
&3\max\{10\alpha + 2, 12\} \sum_{j=\mu_t-M_{\mu_t}}^{t-1} \eta^{t-j-1} \|w_j\|_Q^2\}.
\end{aligned} \tag{21}$$

As discussed below (15), we derived (21) for $t \geq \tilde{\tau}$. For the case of $t < \tilde{\tau}$, note that the following provides a valid upper bound

$$\begin{aligned}
\|\hat{e}_t\|_{P_1}^2 &\leq \max\{12\eta^{M_t} \|\hat{x}_{t-M_t} - x_{t-M_t}\|_{P_2}^2, \\
&3\max\{10\alpha + 2, 12\} \sum_{j=t-M_t}^{t-1} \eta^{t-j-1} \|w_j\|_Q^2\}.
\end{aligned} \tag{22}$$

Due to $\|\cdot\|_{P_2}^2 \leq \lambda_{\max}(P_2, P_1) \|\cdot\|_{P_1}^2$, we obtain the following upper bound for (21)

$$\begin{aligned}
& \|\hat{e}_t\|_{P_1}^2 \\
& \leq \max\{12\eta^{M_t} \lambda_{\max}(P_2, P_1) \|\hat{x}_{t-M_t} - x_{t-M_t}\|_{P_1}^2, \\
& 24\eta^{t-\mu_t+M_{\mu_t}} \lambda_{\max}(P_2, P_1) \|\hat{x}_{\mu_t-M_{\mu_t}} - x_{\mu_t-M_{\mu_t}}\|_{P_1}^2, \\
& 3\max\{10\alpha + 2, 12\} \sum_{j=\mu_t-M_{\mu_t}}^{t-1} \eta^{t-j-1} \|w_j\|_Q^2\}.
\end{aligned}$$

Selecting the horizon length M large enough such that

$$\rho^M := 24\lambda_{\max}(P_2, P_1)\eta^M < 1 \tag{23}$$

with $\rho \in [0, 1)$, noting that $\rho \geq \eta$, and recalling that $t - \mu_t + M_{\mu_t} \geq M_t \geq M$ for all $t \geq \max\{M, \tilde{\tau}\}$, we obtain for all $t \geq \max\{M, \tilde{\tau}\}$

$$\begin{aligned}
\|\hat{e}_t\|_{P_1}^2 &\leq \max\{\rho^{M_t} \|\hat{x}_{t-M_t} - x_{t-M_t}\|_{P_1}^2, \\
&\rho^{t-\mu_t+M_{\mu_t}} \|\hat{x}_{\mu_t-M_{\mu_t}} - x_{\mu_t-M_{\mu_t}}\|_{P_1}^2, \\
&3\max\{10\alpha + 2, 12\} \sum_{j=\mu_t-M_{\mu_t}}^{t-1} \eta^{t-j-1} \|w_j\|_Q^2\}.
\end{aligned} \tag{24}$$

Notice that in case of $\gamma_t = 0$, $\mu_t = t$ and $M_t = t - \mu_t + M_{\mu_t}$, thus the first two terms of the right-hand side of (24) are identical. Consider some time $l \in \mathbb{I}_{[0, M-1]}$. Using (21) if $l \geq \tilde{\tau}$ or (22) if $l < \tilde{\tau}$, we can write

$$\begin{aligned}
\|\hat{e}_l\|_{P_1}^2 &\leq \max\{12\eta^l \|\hat{e}_0\|_{P_2}^2, 24\eta^l \|\hat{e}_0\|_{P_2}^2, \\
&3\max\{10\alpha + 2, 12\} \sum_{j=0}^{l-1} \eta^{l-j-1} \|w_j\|_Q^2\}.
\end{aligned} \tag{25}$$

Next we recursively apply the bound (24) to the first two terms on the right-hand side of (24)⁴. Applying (24) recursively, using (25) when we reach a time instant less than M , and using that $\eta \leq \rho$, we obtain the following bound

$$\begin{aligned}
\|\hat{e}_t\|_{P_1}^2 &\leq \max\{12\rho^t \|\hat{e}_0\|_{P_2}^2, 24\rho^t \|\hat{e}_0\|_{P_2}^2\} \\
&+ 3\max\{10\alpha + 2, 12\} \sum_{j=0}^{t-1} \rho^{t-j-1} \|w_j\|_Q^2.
\end{aligned}$$

Notice that we upper bounded all disturbance terms that result from applying (24) recursively and (25) by the sum of all disturbances over the whole time interval $[0, t - 1]$. Since $\lambda_{\min}(P_1) \|\hat{e}_t\|^2 \leq \|\hat{e}_t\|_{P_1}^2$, $\|\hat{e}_0\|_{P_2}^2 \leq \lambda_{\max}(P_2) \|\hat{e}_0\|^2$, and $\|w_j\|_Q^2 \leq \lambda_{\max}(Q) \|w_j\|^2$ it holds that

$$\begin{aligned}
\|\hat{e}_t\|^2 &\leq 24 \frac{\lambda_{\max}(P_2)}{\lambda_{\min}(P_1)} \rho^t \|\hat{e}_0\|^2 \\
&+ \frac{3\max\{10\alpha + 2, 12\} \lambda_{\max}(Q)}{\lambda_{\min}(P_1)} \sum_{j=0}^{t-1} \rho^{t-j-1} \|w_j\|^2.
\end{aligned}$$

⁴Similar steps using a sum-based formulation are followed in [20, Corollary 1] and [11, Theorem 1].

Using $\sqrt{a+b} \leq \sqrt{a} + \sqrt{b}$ for all $a, b \geq 0$ results in

$$\begin{aligned} \|\hat{e}_t\| &\leq \sqrt{\frac{24\lambda_{\max}(P_2)}{\lambda_{\min}(P_1)}} \sqrt{\rho^t} \|\hat{e}_0\| \\ &+ \sqrt{\frac{3\max\{10\alpha+2, 12\}\lambda_{\max}(Q)}{\lambda_{\min}(P_1)}} \sum_{j=0}^{t-1} \sqrt{\rho^{t-j-1}} \|w_j\| \end{aligned}$$

and concludes the proof. \blacksquare

Theorem 1 shows that the proposed ET-MHE scheme is an RGES estimator. We note that the disturbance gain increases with increasing α . This is to be expected since for larger α , events are triggered less often. On the other hand, the condition on the required horizon length is independent of α . This is crucial since this means that the MHE scheme does not need to be re-designed if the triggering parameter α is changed (see also Remark 5 below). We note that α could also be omitted in the cost function (8). However, then the RGES proof needs to be suitably adapted, which would result in an increase of the minimum horizon length for larger values of α . By including α in the cost function, we obtain a minimum horizon length independent of α as shown in the proof of Theorem 1.

Remark 5: The choice of α is an important consideration for the performance of the proposed estimator. Although we do not explore this further in this paper, it is possible to use a time-varying α_t in the event triggering condition. This could be advantageous because this enables adjusting the sensitivity of the event-triggering condition. For example, it can help reducing excessive triggering at the start due to a poor prior. When using a time-varying α_t , the cost function must be adjusted accordingly. Either a time varying α_t must also be used in the cost function, or alternatively, the cost function can be formulated using the largest value of α_t that will be used at any point in time. This largest value of α_t then determines the bound on the estimation error.

V. ET-MHE WITH VARYING HORIZON LENGTH

In the following, we present a modified version of the ET-MHE scheme proposed in Section III. While the previous NLP (5)-(7) was always explicitly solved with a fixed horizon of length M for $t \geq M$ (compare Remark 1), the following scheme allows to vary the horizon length every time the optimization problem is solved. We show that this allows to establish a tighter bound on the estimation error at the cost of higher computational complexity and a less intuitive set up. This modified ET-MHE scheme uses the same algorithm as Algorithm 1. The only differences between the two methods lie in the definition of the horizon length and the formulation of the cost function, both of which we introduce in the following.

Before specifying the horizon length M_t , it is essential to define $\sigma_t = \max\{\tau \leq t | \gamma_j = 1, \forall j \in [\tau - \min\{\tau, 2M-1\}, \tau]\}$ ⁵, i.e., the most recent time at which $\min\{t, 2M\}$ consecutive events had occurred. We define the horizon length

⁵Note that in Algorithm 1, $\gamma_0 = 1$, and thus σ_t is well defined for all $t \geq 0$.

as ⁶

$$M_t := \min\{t, t - \mu_{t-\delta_t-M}, t - \sigma_t + M\}. \quad (26)$$

The main idea here is as follows. If there is an event at time t , we do not solve the NLP with a fixed horizon M . Instead, the horizon depends on whether there was an event at time $t - M$. If this is the case, we extend the time interval considered in the cost function from $[t - M, t - 1]$ to $[\mu_{t-M}, t - 1]$. Thereby, if multiple consecutive measurements had been transmitted prior to $t - M$, they are additionally taken into account in the optimization problem. The inclusion of σ_t in the definition of the horizon length serves to ensure an upper bound on the maximum potential horizon length even in scenarios with an arbitrarily large number of consecutive events. By (26), less than $2M$ consecutive measurements are considered in the cost function, thus constraining the horizon length to $M_t < 3M$. Although such a scenario is not typically expected, σ_t is incorporated in the horizon length definition to guarantee that it will not become unbounded and ever-increasing.

This choice of horizon length allows for the establishment of a tighter bound on the estimation error and a smaller minimum horizon length as we show below.

Furthermore, the cost function (7) is modified by replacing $\max\{\alpha, 1\}$ with $(\alpha + 1)$, i.e., the cost function is now given by

$$\begin{aligned} &J(\hat{x}_{t-M_t|t}, \hat{w}_{|t}, \hat{y}_{|t}, t) \\ &= 2\eta^{M_t} \|\hat{x}_{t-M_t|t} - \hat{x}_{t-M_t}\|_{P_2}^2 \\ &+ (\alpha + 1) \left(\sum_{j=t-M_t}^{t-1} \eta^{t-j-1} 2\|\hat{w}_{j|t}\|_Q^2 \right. \\ &\quad \left. + \sum_{j \in \mathbb{I}_{[t-M_t, t-1]} \cap K_s} \eta^{t-j-1} \|\hat{y}_{j|t} - y_j\|_R^2 \right). \end{aligned} \quad (27)$$

As discussed below equation (7), both cost function formulations (7) and (27) are applicable to the ET-MHE scheme presented in Section III. In the following we use (27) as the cost function because this formulation allows us to exploit the varying horizon length to obtain a tighter error bound. Before stating the corresponding theorem, we introduce first the following lemma that will be used to prove RGES.

Lemma 1: Let Assumption 1 hold. Consider the ET-MHE scheme (5)-(6), and (27) with the event-triggering condition (14) and with M_t as defined in (26). Then, for all $t \geq 0$, if either $\gamma_t = 0$ or $\gamma_j = 1, \forall j \in [t - \min\{t, M-1\}, t]$, the following holds

$$\begin{aligned} \|\hat{x}_t - x_t\|_{P_1}^2 &\leq 4\eta^{M_t} \|\hat{x}_{t-M_t} - x_{t-M_t}\|_{P_2}^2 \\ &+ (2\alpha + 4) \sum_{j=t-M_t}^{t-1} \eta^{t-j-1} \|w_j\|_Q^2. \end{aligned} \quad (28)$$

Proof: We can apply the same steps as in the proof of Theorem 1 to obtain (15). Now, first consider the case of $\gamma_t = 0$. If $\gamma_t = 0$, i.e., the bound in (14) holds, then the bound in (10) also holds. Note also, that, by (26), if $\gamma_t = 0$ then

⁶Note that if $t - \delta_t - M < \tilde{\tau}$, then $\mu_{t-\delta_t-M}$ is not defined and the definition of M_t reduces to $M_t := \min\{t, t - \sigma_t + M\}$.

$t - M_t = \epsilon_t - M_{\epsilon_t}$. Hence, using Proposition 1, we can upper bound the last term in (15) as follows

$$\begin{aligned} & \sum_{j \in \mathbb{I}_{[t-M_t, t-1]} \setminus K_s} \eta^{t-j-1} \|y_j - \hat{y}_{j|t}^*\|_R^2 \\ & < \alpha \left(2 \sum_{j=t-M_t}^{\epsilon_t-1} \eta^{t-1-j} \|\hat{w}_{j|\epsilon_t}^*\|_Q^2 \right. \\ & \quad \left. + \sum_{j \in \mathbb{I}_{[t-M_t, \epsilon_t-1]} \cap K_s} \eta^{t-1-j} \|\hat{y}_{j|\epsilon_t}^* - y_j\|_R^2 \right) \end{aligned} \quad (29)$$

resulting in

$$\begin{aligned} \|\hat{x}_t - x_t\|_{P_1}^2 & \leq 2\eta^{M_t} \|\hat{x}_{t-M_t} - x_{t-M_t}\|_{P_2}^2 \\ & \quad + 2\eta^{M_t} \|\hat{x}_{t-M_t|t}^* - \hat{x}_{t-M_t}\|_{P_2}^2 \\ & \quad + \sum_{j=t-M_t}^{t-1} \eta^{t-j-1} 2\|w_j\|_Q^2 \\ & \quad + (\alpha + 1) \left(\sum_{j=t-M_t}^{t-\delta_t-1} \eta^{t-j-1} 2\|\hat{w}_{j|t-\delta_t}^*\|_Q^2 \right. \\ & \quad \left. + \sum_{j \in \mathbb{I}_{[t-M_t, t-\delta_t-1]} \cap K_s} \eta^{t-j-1} \|\hat{y}_{j|t-\delta_t}^* - y_j\|_R^2 \right). \end{aligned}$$

Recalling the choice of our cost function, we can equivalently write

$$\begin{aligned} \|\hat{x}_t - x_t\|_{P_1}^2 & \leq 2\eta^{M_t} \|\hat{x}_{t-M_t} - x_{t-M_t}\|_{P_2}^2 \\ & \quad + \sum_{j=t-M_t}^{t-1} 2\eta^{t-j-1} \|w_j\|_Q^2 \\ & \quad + J(\hat{x}_{t-M_t|t}^*, \hat{w}_{\cdot|t}^*, \hat{y}_{\cdot|t}^*, t). \end{aligned}$$

Since $J(\hat{x}_{t-M_t|t}^*, \hat{w}_{\cdot|t}^*, \hat{y}_{\cdot|t}^*, t) \leq J(x_{t-M_t}, w_{\cdot|t}, y_{\cdot|t}, t)$ by optimality, the inequality in (28) holds as desired.

If $\gamma_j = 1$, $\forall j \in [t - \min\{t, M - 1\}, t]$, then by (26) the optimization problem is solved over a horizon $M_t < 2M$ with measurements available at every time instant in the horizon, i.e., $\tau \in K_s$ for all $\tau \in [t - M_t, t - 1]$. (Recall that if $\gamma_\tau = 1$ then $y_{\tau-1}$ is transmitted.) Hence, the last term of (15) is zero and we can directly obtain (28) without the intermediate step (29). ■

Theorem 2 (RGES of ET-MHE with varying M_t): Let Assumption 1 hold and $M \in \mathbb{I}_{\geq 0}$ be chosen such that $8\lambda_{\max}(P_2, P_1)\eta^M < 1$. Then there exists $\rho \in [0, 1)$ such that the state estimation error of the ET-MHE scheme (5)-(6) and (27) with the even-triggering condition (14) and with M_t as defined in (26) satisfies for all $t \geq 0$

$$\begin{aligned} \|\hat{e}_t\| & \leq \sqrt{\frac{8\lambda_{\max}(P_2)}{\lambda_{\min}(P_1)}} \sqrt{\rho^t} \|\hat{e}_0\| \\ & \quad + \sqrt{\frac{(10\alpha + 12)\lambda_{\max}(Q)}{\lambda_{\min}(P_1)}} \sum_{j=0}^{t-1} \sqrt{\rho^{t-j-1}} \|w_j\|, \end{aligned} \quad (30)$$

i.e., the ET-MHE is an RGES estimator according to Definition 1.

Proof: We can apply the same arguments from the proof of Theorem 1 up to (21), to obtain

$$\begin{aligned} \|\hat{e}_t\|_{P_1}^2 & \leq 4\eta^{M_t} \|\hat{x}_{t-M_t} - x_{t-M_t}\|_{P_2}^2 \\ & \quad + 8\eta^{t-\mu_t+M_{\mu_t}} \|\hat{x}_{\mu_t-M_{\mu_t}} - x_{\mu_t-M_{\mu_t}}\|_{P_2}^2 \\ & \quad + (2\alpha + 4) \sum_{j=t-M_t}^{t-1} \eta^{t-j-1} \|w_j\|_Q^2 \\ & \quad + (8\alpha + 8) \sum_{j=\mu_t-M_{\mu_t}}^{\mu_t-1} \eta^{t-j-1} \|w_j\|_Q^2. \end{aligned}$$

Consider some time $t > M$ for some M such that

$$\rho^M := 8\lambda_{\max}(P_2, P_1)\eta^M < 1 \quad (31)$$

with $\rho \in [0, 1)$. Due to $\|\hat{e}_{\tau-M_\tau}\|_{P_2}^2 \leq \lambda_{\max}(P_2, P_1)\|\hat{e}_{\tau-M_\tau}\|_{P_1}^2$, (31) and $\rho \geq \eta$, we can write

$$\begin{aligned} \|\hat{e}_t\|_{P_1}^2 & \leq \rho^{M_t} \|\hat{x}_{t-M_t}\|_{P_1}^2 + \rho^{t-\mu_t+M_{\mu_t}} \|\hat{x}_{\mu_t-M_{\mu_t}}\|_{P_1}^2 \\ & \quad + (2\alpha + 4) \sum_{j=t-M_t}^{t-1} \eta^{t-j-1} \|w_j\|_Q^2 \\ & \quad + (8\alpha + 8) \sum_{j=\mu_t-M_{\mu_t}}^{\mu_t-1} \eta^{t-j-1} \|w_j\|_Q^2. \end{aligned} \quad (32)$$

By definition of M_t in (26) we know that either $\gamma_{t-M_t} = 0$ or $\gamma_j = 1$, $\forall j \in [t - M_t - \min\{t - M_t, M - 1\}, t - M_t]$ and, moreover, that either $\gamma_{\mu_t-M_{\mu_t}} = 0$ or $\gamma_j = 1$, $\forall j \in [\mu_t - M_{\mu_t} - \min\{\mu_t - M_{\mu_t}, M - 1\}, \mu_t - M_{\mu_t}]$, and thus Lemma 1 is applicable. Using again $\|\hat{e}_{\tau-M_\tau}\|_{P_2}^2 \leq \lambda_{\max}(P_2, P_1)\|\hat{e}_{\tau-M_\tau}\|_{P_1}^2$, (31) and $\rho \geq \eta$, (28) can be upper bounded for $\tau \geq M$ by

$$\begin{aligned} \|\hat{x}_\tau - x_\tau\|_{P_1}^2 & \leq \rho^{M_\tau} \|\hat{x}_{\tau-M_\tau} - x_{\tau-M_\tau}\|_{P_1}^2 \\ & \quad + (2\alpha + 4) \sum_{j=\tau-M_\tau}^{t-1} \rho^{t-j-1} \|w_j\|_Q^2. \end{aligned} \quad (33)$$

By recursively applying (33) to the first two terms on the right-hand side of (32), using (28) upon reaching a time instance less than M , and considering that $\eta \leq \rho$, we derive the following bound

$$\|\hat{e}_t\|_{P_1}^2 \leq 8\rho^t \|\hat{e}_0\|_{P_2}^2 + (10\alpha + 12) \sum_{j=0}^{t-1} \rho^{t-j-1} \|w_j\|_Q^2.$$

Performing reformulations analogously to the steps in the proof of Theorem 1, we finally obtain (30). ■

Due to the new definition of the horizon length in (26) the bound derived in Lemma 1 can be recursively applied in the proof above. This allows to transition from (32) to (33) without the need to use a max-based bound as in the proof of Theorem 1 (compare the last inequality in (21)). This results in a smaller error bound and minimum horizon length.

The discussion following the proof of Theorem 1 remains valid for this modified ET-MHE scheme with varying horizon length.

While extending the ET-MHE scheme from Section III to allow a varying horizon length enables the derivation of a smaller error bound and a smaller minimal required horizon

length (compare Theorem 2 with Theorem 1), the original scheme in Section III remains simpler to implement and computationally less demanding. This is due to the use of the fixed horizon length, which avoids the need to determine the horizon length at each event and allows the optimization problem to retain a constant structure throughout.

VI. NUMERICAL EXAMPLES

In this section we present simulation examples for the ET-MHE scheme from Section III⁷. Furthermore, we also discuss the influence of the additional constraint (6) on the estimation results and the modified scheme with varying horizon length.

A. Example 1: Batch reactor

In the first example consider the following system

$$\begin{aligned} x_{1,t+1} &= x_{1,t} + \tau(-2k_1 x_{1,t}^2 + 2k_2 x_{2,t}) + w_{1,t}, \\ x_{2,t+1} &= x_{2,t} + \tau(k_1 x_{1,t}^2 - k_2 x_{2,t}) + w_{2,t}, \\ y &= x_{1,t} + x_{2,t} + w_{3,t} \end{aligned}$$

with $k_1 = 0.16$, $k_2 = 0.0064$, and sampling time $\tau = 0.1$. This corresponds to a batch reactor system from [23] using an Euler discretization. This example has become a standard benchmark in the MHE literature (e.g. in [19], [20]), since other nonlinear state estimators such as the extended Kalman filter often fail to yield meaningful results. We consider $x_0 = [3, 1]^\top$ and the poor initial estimate $\hat{x}_0 = [0.1, 4.5]^\top$. In the simulation, the additional disturbance $w \in \mathbb{R}^3$ is treated as a uniformly distributed random variable that satisfies $|w_i| \leq 10^{-3}$, $i = 1, 2$, and $|w_3| \leq 0.1$.

For parameterizing the cost function, we use the parameters of the quadratic Lyapunov function $W_\delta = \|x - \tilde{x}\|_P^2$ computed in [20] where

$$P = \begin{bmatrix} 4.539 & 4.171 \\ 4.171 & 3.834 \end{bmatrix}, \quad Q = \begin{bmatrix} 10^3 & 0 & 0 \\ 0 & 10^4 & 0 \\ 0 & 0 & 10^3 \end{bmatrix}, \quad R = 10^3,$$

$P_1 = P_2 = P$ and the decay rate $\eta = 0.91$. These parameters satisfy Assumption 1. Using condition (23) we obtain a minimal horizon length of $M_{\min} = 34$ guaranteeing robust stability of the ET-MHE. In Figure 2, an exemplary simulation for $\alpha = 5$ is shown. It can be observed that the trajectories of the estimated state for $\alpha = 5$ and $\alpha = 0$ (where $\alpha = 0$ implies that an event was triggered at every time instance, effectively functioning as a Moving Horizon Estimation (MHE) without event-triggering) are almost identical. In Figure 3 the corresponding values of γ_t are plotted, i.e. the time instances when an event was scheduled are displayed.

Next, we consider different values of α between 1 and 14. For each value of α we performed 200 simulations with different disturbance sequences. As expected, larger values of α result in fewer events being triggered. This correlation is illustrated in Figure 4.

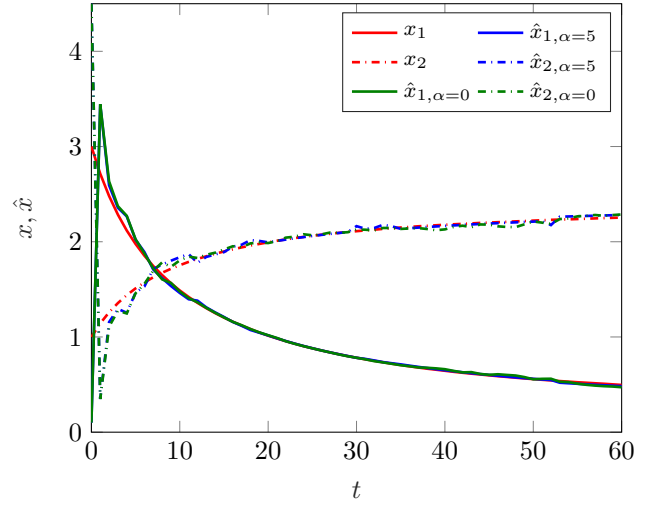


Fig. 2. Comparison of ET-MHE results for $\alpha = 5$, MHE estimates (without event-triggering, i.e., $\alpha = 0$) and real system states.

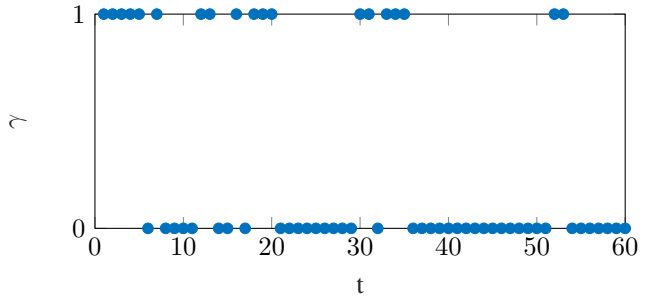


Fig. 3. Event scheduling variable γ for simulation with $\alpha = 5$.

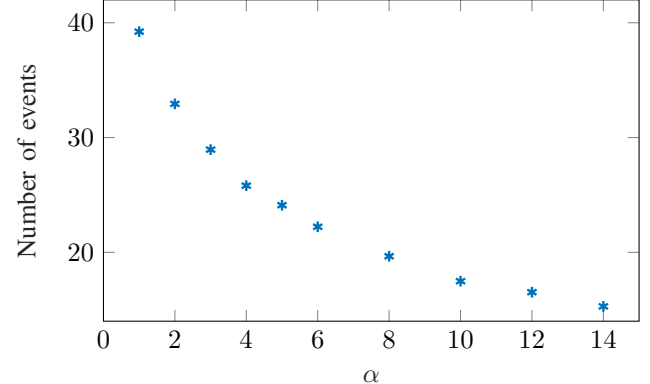


Fig. 4. Average number of events for different choices of α for Example 1 (batch reactor), simulated over 60 time steps (i.e., 6 seconds).

B. Example 2: Robot Arm

As a second example we consider a two-link robot arm moving in a 2D-plane as depicted in Figure 5. For the description of the dynamics see e.g. [12, Example 3.2-2]. The system state is defined as $x = [\theta_1, \theta_2, \dot{\theta}_1, \dot{\theta}_2]^\top$, with the measurement output given by $y = [\theta_1, \theta_2]^\top$. Each link of the arm is assumed to have a mass of 1 kg and a length of 1 m. We applied again an Euler discretization with

⁷Matlab code available at <https://doi.org/10.25835/vwaa7o0s>

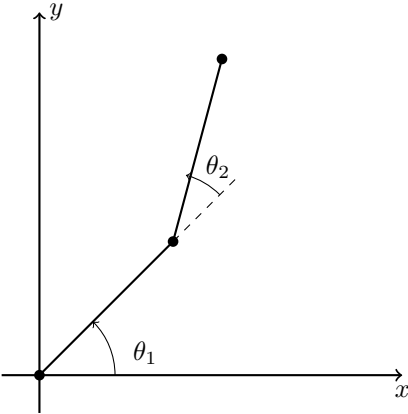


Fig. 5. Two-link robot arm moving in a 2D-plane.

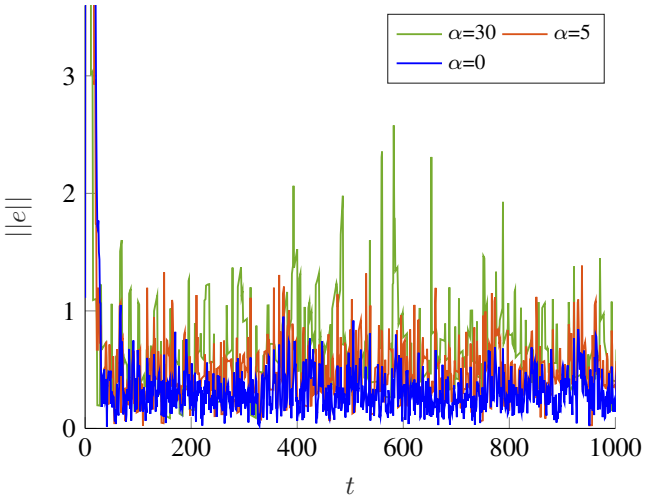


Fig. 6. Estimation error over time for simulation of robot arm with different values of α .

the sampling time $\tau = 0.005$. We consider additive process and measurement noise $w = [w_1, w_2, w_3, w_4, w_5, w_6]^\top$. The initial conditions are set as $x_0 = [\pi/4, \pi/4, 0, 0]^\top$ and $\bar{x}_0 = [0, 0, 0, 0]^\top$. For parameterizing the cost function, a quadratic Lyapunov function is computed following the procedure in [20], with a decay rate of $\eta = 0.85$.

In the following simulation we consider a uniformly distributed process noise and measurement noise that satisfy $|w_i| \leq 0.01$, $i = 1, 2, 3, 4$ and $|w_i| \leq 0.05$, $i = 5, 6$, respectively. Figure 6 displays the estimation error for $\alpha = 5$ and $\alpha = 30$ as well as for $\alpha = 0$, i.e., the non-event-triggered case. The estimation error consistently converges to a region near zero. Furthermore, Table I presents the root mean square estimation error averaged over 100 simulations for $\alpha \in \{0, 5, 10, 15, 20, 30, 40, 50, 60\}$ and for two different measurement noise levels ($|w_i| \leq 0.05$ and $|w_i| \leq 0.1$, $i = 5, 6$). Both Figure 6 and Table I show that, as expected, a smaller α , i.e., more frequent measurement transmission, results in a smaller estimation error. This behavior aligns with our theoretical findings regarding the error bound (cf. Theorem 1).

In Figure 7, the average number of events for $\alpha \in \{5, 10, 15, 20, 30, 40, 50, 60\}$ is presented. As with the first

TABLE I
AVERAGE ROOT MEAN SQUARE STATE ESTIMATION ERROR FOR DIFFERENT VALUES OF α

α	RMSE	
	$ w_i \leq 0.05, i = 5, 6$	$ w_i \leq 0.1, i = 5, 6$
0	0.5167	0.8161
5	0.6166	1.0101
10	0.6414	1.0855
15	0.6561	1.1225
20	0.6661	1.1497
30	0.6710	1.1951
40	0.6795	1.2295
50	0.6899	1.2461
60	0.6918	1.2747

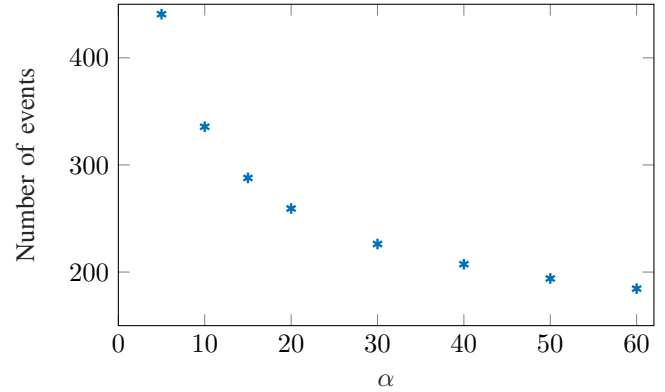


Fig. 7. Average number of events for different choices of α for Example 2 (robot arm), simulated over 1000 time steps (i.e., 5 seconds).

example, an increase in α results in a decrease in the number of events.

C. Additional constraint of MHE's NLP

After having tested the functionality of the algorithm with these two examples, we now examine the impact of the additional constraint (6) on the simulation results. The inclusion of this constraint generally had no significant effect on the resulting estimation error in the conducted simulations. Specifically, we performed 2000 simulations for the batch reactor example (200 different disturbance sequences for each $\alpha \in \{1, 2, 3, 4, 5, 6, 8, 10, 12, 14\}$). For the robot arm we conducted 1600 simulations, namely 200 simulations per $\alpha \in \{5, 10, 15, 20, 30, 40, 50, 60\}$, using 100 different disturbance sequences for each of the two measurement noise levels ($|w_i| \leq 0.1$, $|w_i| \leq 0.05$, $i = 5, 6$). In a substantial number of instances, the additional constraint either did not affect the solution to the optimization problem (36 % (batch reactor) and 13 % (robot arm)) or led to a slight reduction in the estimation error (49 % (batch reactor) and 57 % (robot arm)). However, as mentioned previously, even when the constraint did influence the results, the difference in estimation error remained negligibly small. Therefore, one can conclude that incorporating this constraint into the optimization problem is not restrictive. While it serves to establish our theoretical guarantees, its practical impact is minimal.

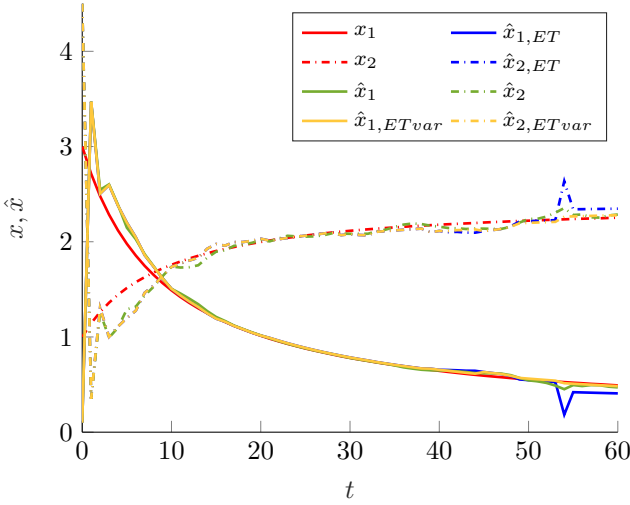


Fig. 8. Comparison of ET-MHE results for $\alpha = 5$ using a fixed or varying horizon length (blue and yellow, respectively), MHE estimates without event-triggering, i.e., $\alpha = 0$ (green) and real system states (red).

D. Comparison with ET-MHE using a varying horizon length

In the following, we briefly discuss the modified algorithm presented in Section V that utilizes a varying horizon length. We conducted again the 2000 simulations of the batch reactor and the 1600 simulations of the robot arm as described in the paragraph above using the ET-MHE with varying horizon length. For the batch reactor, in 77% of the simulations, the ET-MHE with a varying horizon length resulted in a smaller estimation error. The average improvement was approximately 1%, indicating a minor benefit, though improvements were as high as 15% in some instances. In case of the robot arm, in 80% of the simulations, the estimation error was smaller when employing the ET-MHE with a varying horizon length. On average, the improvement was about 3%, and improvements reached up to 21% in certain cases. Overall, the improvement achieved by using the ET-MHE scheme with a varying horizon length remains, on average, relatively small. Nevertheless, in individual situations, we could observe a considerable advantage of this approach, as illustrated in the following example.

Figure 8 illustrates a simulation in which the estimation error is significantly reduced when employing the proposed scheme with a varying horizon length. For the majority of the simulation, the estimated trajectories obtained from both the ET-MHE scheme with the fixed horizon length and the version with a varying horizon closely match. However, towards the end of the simulation, a notable deviation occurs. At $t = 54$, the estimate from the fixed-horizon scheme becomes inaccurate, whereas the varying-horizon scheme still provides a good estimate. A plausible interpretation of this behavior is that, at $t - M = 54 - 34 = 20$, a large number of consecutive events had occurred at the preceding time steps (see Figure 9) and thus, the varying horizon scheme considered significantly more output information in the optimization problem, enabling a more reliable estimate at this point.

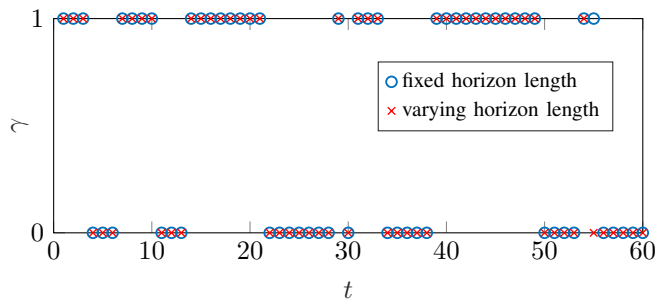


Fig. 9. Event scheduling variable γ for the experiment in Figure 8.

VII. CONCLUSION

This paper presents an event-triggered moving horizon state estimator. The even-triggering condition and the optimization problem of the MHE are designed such that the optimization problem only needs to be solved if an event is scheduled and such that only a single measurement needs to be transmitted. When an event occurs, the current state estimate is obtained by solving the MHE's NLP, while open-loop predictions are used to compute state estimates between events. Additionally, we demonstrated that if the system is exponentially i-IOSS, the proposed ET-MHE achieves robust global exponential stability. Furthermore, we also showed that with the adoption of a varying horizon length, a tighter bound on the estimation error can be achieved. The effectiveness of the proposed ET-MHE scheme was illustrated through two numerical examples. Future research could explore adapting the ET-MHE framework for networked control systems with multiple interconnected components, where the efficient sharing and distribution of limited resources become crucial.

REFERENCES

- [1] I.F. Akyildiz, W. Su, Y. Sankarasubramaniam, E. Cayirci, "Wireless sensor networks: a survey," *Computer Networks*, vol. 38, no. 4, pp. 393-422, 2002.
- [2] D. A. Allan and J. B. Rawlings, "Moving horizon estimation" *Handbook of model predictive control*, pp. 99-124, Cham: Springer International Publishing, 2018.
- [3] D. A. Allan, J. B. Rawlings, and A. R. Teel, "Nonlinear detectability and incremental input/output-to-state stability," *TWCCC Technical Report 2020-01*, 2020.
- [4] D. A. Allan and J. B. Rawlings, "Robust Stability of Full Information Estimation," *SIAM Journal on Control and Optimization*, vol. 59, no. 5, pp. 3472-3497, 2021.
- [5] L. Etienne and S. D. Gennaro, "Event-triggered observation of nonlinear Lipschitz systems via impulsive observers," *IFAC-PapersOnLine*, vol. 49, no. 18, pp. 666-671, 2016.
- [6] X. Ge, Q.-L. Han, X.-M. Zhang, L. Ding and F. Yang, "Distributed Event-Triggered Estimation Over Sensor Networks: A Survey," *IEEE Transactions on Cybernetics*, vol. 50, no. 3, pp. 1306-1320, 2020.
- [7] L. Ji, J. B. Rawlings, W. Hu, A. Wynn and M. Diehl, "Robust Stability of Moving Horizon Estimation Under Bounded Disturbances," *IEEE Transactions on Automatic Control*, vol. 61, no. 11, pp. 3509-3514, 2016.
- [8] S. Knüfer and M. A. Müller, "Robust Global Exponential Stability for Moving Horizon Estimation," *57th IEEE Conference on Decision and Control (CDC)*, pp. 3477-3482, 2018.
- [9] S. Knüfer and M. A. Müller, "Time-Discounted Incremental Input/Output-to-State Stability," *59th IEEE Conference on Decision and Control (CDC)*, pp. 5394-5400, 2020.

- [10] S. Knüfer and M. A. Müller, "Nonlinear full information and moving horizon estimation: Robust global asymptotic stability," *Automatica*, 150:110603, 2023.
- [11] I. Krauss, J. D. Schiller, V. G. Lopez and M. A. Müller, "Event-triggered moving horizon estimation for nonlinear systems," *IEEE 63rd Conference on Decision and Control (CDC)*, pp. 3801-3806, 2024.
- [12] F. L. Lewis, D. M. Dawson and C. T. Abdallah, *Robot Manipulator Control Theory and Practice*, 2nd ed., rev. and expanded, Marcel Dekker, 2004.
- [13] S. Li, Z. Li, J. Li, T. Fernando, H. H.-C. Iu, Q. Wang and X. Liu, "Application of Event-Triggered Cubature Kalman Filter for Remote Nonlinear State Estimation in Wireless Sensor Network," *IEEE Transactions on Industrial Electronics*, vol. 68, no. 6, pp. 5133-5145, 2021.
- [14] Z. Li, S. Li, B. Liu, S. S. Yu and P. Shi, "A Stochastic Event-Triggered Robust Cubature Kalman Filtering Approach to Power System Dynamic State Estimation With Non-Gaussian Measurement Noises," *IEEE Transactions on Control Systems Technology*, vol. 31, no. 2, pp. 889-896, 2023.
- [15] Z. Li, B. Xue and Y. Chen, "Event-Triggered State Estimation for Uncertain Systems with Binary Encoding Transmission Scheme," *Mathematics*, vol. 11, no. 17, 2023.
- [16] L. Li, D. Yu, Y. Xia and H. Yang, "Remote Nonlinear State Estimation With Stochastic Event-Triggered Sensor Schedule," *IEEE Transactions on Cybernetics*, vol. 49, no. 3, pp. 734-745, 2019.
- [17] M. A. Müller, "Nonlinear moving horizon estimation in the presence of bounded disturbances," *Automatica*, vol. 79, pp. 306-314, 2017.
- [18] C. Peng, F. Li, "A survey on recent advances in event-triggered communication and control," *Information Sciences*, vol. 457-458, pp. 113-125, 2018.
- [19] J. B. Rawlings, D. Q. Mayne and M. M. Diehl, *Model Predictive Control: Theory, Computation and Design*, 2nd ed. Santa Barbara, CA, USA: Nob Hill Publishing LLC, 2022, 4th printing.
- [20] J. D. Schiller, S. Muntwiler, J. Köhler, M. N. Zeilinger and M. A. Müller, "A Lyapunov function for robust stability of moving horizon estimation," *IEEE Transactions on Automatic Control*, vol. 68, no. 12, pp. 7466-7481, 2023.
- [21] D. Shi, T. Chen, L. Shi, "Event-triggered maximum likelihood state estimation," *Automatica*, Vol. 50, no. 1, pp. 247-254, 2014.
- [22] C. Song, H. P. Wang, Y. Tian, and G. Zheng, "Event-triggered observer design for output-sampled systems," *Nonlinear Analysis: Hybrid Systems*, vol. 43, 2021.
- [23] M. J. Tenny and J. B. Rawlings, "Efficient moving horizon estimation and nonlinear model predictive control," *Proceedings of the 2002 American Control Conference*, vol.6, pp. 4475-4480, 2002.
- [24] X. Yin and J. Liu, "Event-Triggered State Estimation of Linear Systems Using Moving Horizon Estimation," *IEEE Transactions on Control Systems Technology*, vol. 29, no. 2, pp. 901-909, 2021.
- [25] L. Zou, Z. Wang and D. Zhou, "Moving horizon estimation with non-uniform sampling under component-based dynamic event-triggered transmission," *Automatica*, vol. 120, 2020.
- [26] L. Zou, Z. Wang, Q. -L. Han and D. Zhou, "Moving Horizon Estimation of Networked Nonlinear Systems With Random Access Protocol," in *IEEE Transactions on Systems, Man, and Cybernetics: Systems*, vol. 51, no. 5, pp. 2937-2948, 2021.



Victor G. Lopez (Member, IEEE) received his B.Sc. degree in Communications and Electronics Engineering from the Universidad Autonoma de Campeche, in Campeche, Mexico, in 2010, the M.Sc. degree in Electrical Engineering from the Research and Advanced Studies Center (Cinvestav), in Guadalajara, Mexico, in 2013, and his PhD degree in Electrical Engineering from the University of Texas at Arlington, Texas, USA, in 2019. In 2015 Victor was a Lecturer at the Western Technological Institute of Superior Studies (ITESO) in Guadalajara, Mexico. From August 2019 to June 2020, he was a postdoctoral researcher at the University of Texas at Arlington Research Institute and an Adjunct Professor in the Electrical Engineering department at UTA. Victor is currently a postdoctoral researcher at the Institute of Automatic Control, Leibniz University Hanover, in Hanover, Germany. His research interest include cyber-physical systems, reinforcement learning, game theory, distributed control and robust control.



Matthias A. Müller (Senior Member, IEEE) received a Diploma degree in engineering cybernetics from the University of Stuttgart, Germany, an M.Sc. in electrical and computer engineering from the University of Illinois at Urbana-Champaign, US (both in 2009), and a Ph.D. from the University of Stuttgart in 2014. Since 2019, he is Director of the Institute of Automatic Control and Full Professor at the Leibniz University Hannover, Germany.

His research interests include nonlinear control and estimation, model predictive control, and data- and learning-based control, with application in different fields including biomedical engineering and robotics. He has received various awards for his work, including the 2015 European Systems & Control PhD Thesis Award, the inaugural Brockett-Willems Outstanding Paper Award for the best paper published in Systems & Control Letters in the period 2014-2018, an ERC starting grant in 2020, the IEEE CSS George S. Axelby Outstanding Paper Award 2022, and the Journal of Process Control Paper Award 2023. He serves/d as an associate editor for *Automatica* and as an editor of the International Journal of Robust and Nonlinear Control.



Isabelle Krauss received her Master degree in Automation Engineering from RWTH Aachen University, Germany, in 2020. Since then, she has been a research assistant at the Institute of Automatic Control, Leibniz University Hannover, Germany, where she is currently working on her Ph.D. under the supervision of Prof. Matthias A. Müller. Her research interests are in the area of observability and state estimation with focus on nonlinear systems.